IL NUOVO CIMENTO **44 C** (2021) 10
DOI 10.1393/ncc/i2021-21010-1

COMMUNICATIONS: SIF Congress 2020

Gravitational wave cosmology with galaxy surveys

A. PALMESE([1])([2])([*])

([1]) *Fermi National Accelerator Laboratory - P. O. Box 500, Batavia, IL 60510, USA*
([2]) *Kavli Institute for Cosmological Physics, University of Chicago - Chicago, IL 60637, USA*

received 1 February 2021

Summary. — This paper is based on my presentation at the 106° National Congress of the Italian Physical Society in September 2020. In the talk, I presented the latest cosmological measurements of the Hubble constant H_0 using gravitational wave (GW) standard sirens. Due to the lack of GW events with an associated electromagnetic counterpart apart from GW170817, we have used the *dark* standard siren method, that does not rely on counterparts but uses galaxies' positions from galaxy surveys instead. Using data from the Dark Energy Survey (DES), the standard siren analysis using three GW events (GW170814, GW170817, GW190814) yields $H_0 = 72.0^{+12}_{-8.2}$ km s^{-1} Mpc^{-1} (68% Highest Density Interval). Analyses of future gravitational wave events from the next LIGO/Virgo/KAGRA observing run using the statistical standard siren method and a DES–like galaxy catalog are expected to bring even more precise constraints on H_0, at the level of $\sim$ 2–5% (statistical) precision after $\sim$ 200 GW detections at a distance of $<$ 900 Mpc. Next-generation GW detectors will also provide precise enough GW measurements that their detections, together with a galaxy survey like the Dark Energy Spectroscopic Instrument (DESI), will be able to place precise constraints on the growth of large-scale structure and on gravity models.

1. – Introduction

The first detection of gravitational waves (GW) in 2015 by the Laser Interferometer Gravitational-wave Observatory (LIGO), and later the discovery of the first electromagnetic (EM) counterpart to a gravitational-wave event (GW170817; [1, 2]), have triggered a vast number of observations across multiple experiments, opening new horizons for understanding topics ranging from the recent expansion of the Universe to stellar evolution (*e.g.*, [3-6]). A very promising application of GW observations is that of standard siren analyses [7]. A GW detection provides a measurement of the luminosity distance,

([*]) E-mail: palmese@fnal.gov

and if an independent measurement of the redshift is available, for example from its host galaxy, it is possible to infer cosmological parameters through the distance-redshift relation. Nearby GW detections ($z < 0.1$), such as those that are more easily detectable by the current-generation (*i.e.*, 2G) GW detectors, are mostly sensitive to the Hubble constant H_0 through the distance-redshift relation.

Inferring the Hubble constant has become of particular interest in the latest years since leading measurements of H_0 from different cosmological probes have come to a 4.4σ tension. Independent measurements of the same parameter can shed light on the origin of this discrepancy, which could potentially be an indication for new physics. Gravitational waves have the potential to help us understand the Hubble tension (*e.g.*, [8,9]), and that potential is exploited when GW observations are combined with electromagnetic data, including photons at all observable wavelengths. In my talk at the 106 Italian Physical Society (SIF) Congress, I have shown how combination of GW events with optical data from recent and upcoming large galaxy surveys, can provide competitive constraints on cosmological parameters.

2. – Gravitational wave standard sirens

In the ideal case, an electromagnetic (EM) counterpart to a gravitational-wave event is discovered, allowing the identification of a unique host galaxy whose redshift can be used in a standard siren measurement, which we can refer to as a "bright standard siren". Only one confident bright standard siren measurement exists to date, and it comes from the binary neutron star (BNS) merger GW170817 [3]. Counterparts are proving to be rare, as they are usually only expected to come from compact object mergers that contain at least one neutron star, while the vast majority of current GW detections come from binary black hole (BBH) mergers. When a counterpart is not available, the GW localization is usually so large that it would be consistent with several, in most cases thousands or even hundreds of thousands, possible host galaxies. For the most well-localized events, which are usually also the closest in distance, and therefore, the most sensitive to H_0, it is possible to apply a "dark" or "statistical" standard siren method (which is what was initially conceived for this method by Schutz [7]) that takes into account all potential host galaxies within a statistical framework, through a marginalization over those galaxies. This method provides H_0 constraints that are less precise than those from bright sirens when a single event is considered, but the events without counterpart outnumber those with counterpart by a factor of $\mathcal{O}(10)$, so that both methods are promising cosmological probes.

2˙1. *Current measurements.* – In a recent work made with the Dark Energy Survey (DES; [10]) Collaboration, the LIGO Scientific Collaboration, and the Virgo Collaboration, we have produced the first measurement of the Hubble constant from a binary black hole merger, using the dark standard siren method [11]. The GW data comes from the LIGO/Virgo GW event GW170814 [12], while the galaxies' data come from the DES imaging data. The redshift information for the galaxies is derived through photometric redshift estimation using neural networks. For a prior in H_0 uniform between $[20, 140]$ km s^{-1} Mpc^{-1}, the analysis yields 77^{+41}_{-33} km s^{-1} Mpc^{-1} (maximum *a posteriori* and 68% Highest Density Interval, HDI). This analysis was an important proof of principle for future dark siren measurements, and it showed the importance of having a complete and uniform galaxy catalog across the high-probability region of the gravitational-wave event.

During the third observing run (O3) by LIGO and Virgo, an even more promising dark standard siren has been detected, GW190814 [13]. This event, a likely binary black hole, has been followed up with the deepest imaging (*e.g.*, [14]), but no counterpart has been detected. With a localization comoving volume of 3.2×10^4 Mpc^3 (90% credible interval, CI), GW190814 is the second to best localized amongst all GW events detected so far, only second to the bright standard siren GW170817, so that GW190814 is the best dark siren available. Like GW170814, the GW190814 90% CI volume is also fully covered by the wide and deep DES data, as can be seen in the left panel of fig. 1. The wealth of the DES data and its overlap with various spectroscopic datasets allowed us to fully characterize photometric redshift systematic uncertainties and biases for the first time in a standard siren analysis. We also take advantage of the full redshift probability density function (PDF) of single galaxies to better recover the galaxies' redshift distribution along the line of sight of the GW event, which is the relevant redshift information utilized in the dark siren measurement. We also marginalize over possible redshift dependent biases arising from the photometric redshifts. The final DES dark siren H_0 posterior from a combination of GW170814 and GW190814 is shown by the dark solid grey curve in the right plot of fig. 1, and yields $H_0 = 77^{+41}_{-22}$ km s^{-1} Mpc^{-1} (maximum *a posteriori* and 68% HDI), using a flat H_0 prior in the range [20,140] km s^{-1} Mpc^{-1}. Finally, a combination of GW170814, GW190814 and GW170817 yields $H_0 = 72.0^{+12}_{-8.2}$ km s^{-1} Mpc^{-1}, where we use the bright standard siren posterior from [15] with our prior. The addition of GW190814 and GW170814 to GW170817 improves the 68% CI interval by $\sim 18\%$, showing how well-localized GW events without counterparts can provide a substantial contribution to standard siren measurements, provided that a complete and uniform galaxy catalog is available at the merger's location.

2˙2. *Prospects*. – We consider two types of simulations that allow us to make predictions for future standard siren measurements using LIGO/Virgo events and DES

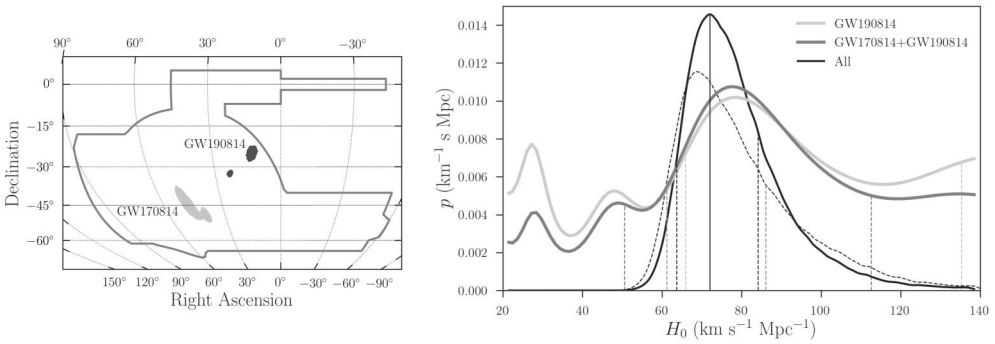

Fig. 1. – Left: 90% CI sky localization area of the binary black hole merger events GW170814 and GW190814. The contour line shows the footprint of the DES observations. Right: Hubble constant posterior probability distribution functions from the standard siren analysis presented. The two grey solid lines show the posterior resulting from a statistical standard siren analysis of GW190814 alone (lighter grey) and from a combination of GW190814 and GW170814 (darker grey). The dotted line is the posterior from the bright standard siren analysis of GW170817 from [15], that includes a more sophisticated treatment of the host galaxy peculiar velocity compared to previous works. The black line is the posterior from the combination of all aforementioned standard sirens. Vertical lines indicate the 68% HDI for each posterior. Adapted from [16].

(or DES-like) galaxy catalogs. The first type of simulation consists in rotating existing events with no counterpart on top of the DES footprint, in order to predict the precision that could be reached with existing events if a DES-like catalog is present (or will be produced) in these regions. We select the top 20 events from O1, O2 and O3, based on their 90% CI comoving volume, and after removing GW170814, GW170817 and GW190814, we disregard events that cannot be fit in the DES area. This selection leaves us with 13 events to rotate. We find that a combination of these events could provide a $\sim 30\%$ improvement on the dark siren measurement of H_0. While this would be a significant improvement, new events from the upcoming LIGO/Virgo (and KAGRA) runs are expected to provide even more exciting results.

For the second type of simulation, we use `BAYESTAR` [17]. We inject BBH events out to 900 Mpc, assuming a rate that is uniform in comoving volume and a flat ΛCDM cosmology with $H_0 = 70$ km/s/Mpc and $\Omega_m = 0.286$. We then consider LIGO/Virgo detections of such events at design sensitivity (*i.e.*, an O4 run, expected to start in ~ 2022). The single detector SNR-threshold assumed is 4, while the network SNR-threshold is 12, and a detection is only considered if it triggered at least two detectors. This selection produces a sample of 192 BBH. The real and simulated maps are rotated on a DES galaxy at the redshift of the event, provided $H_0 = 70$ km/s/Mpc in a flat ΛCDM scenario. The position of the highest probability pixel is moved with respect to the assigned host by an amount that follows the angular probability from the skymap fig. 2 shows the H_0 posterior from the simulated BBH events, showing how after combining $\mathcal{O}(100)$ events the input cosmology (dashed line) is recovered with 2–5% statistical precision. Such sample of BBH events is expected to be available a few years-long run by LIGO/Virgo at design sensitivity, so preliminary results of this kind could be be possible towards 2024–2025. In combination with bright standard sirens [8, 18], the $\sim 2\%$ precision required to understand the Hubble tension is expected to be reached within this time frame.

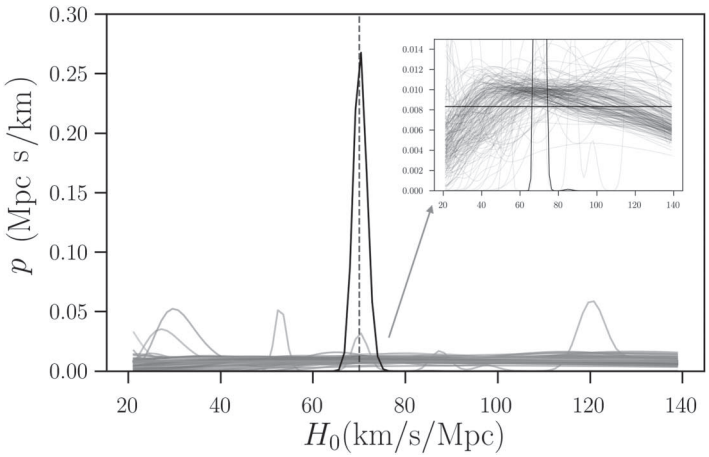

Fig. 2. – Dark standard siren constraints forecast. Posterior probability for H_0 from 200 BBH events out to 900 Mpc from LIGO at design sensitivity, simulated on top of a DES-like galaxy catalog. Grey lines are for single events, the black line is from the combination of all events. The zoomed insert shows how, despite the apparent flatness of single event posteriors, they all have support around the input value of $H_0 = 70$ km/s/Mpc (vertical dotted line).

3. – Probing the Universe's growth of structure and gravity with peculiar velocities and gravitational waves

Galaxies' peculiar velocities arise from the motion of galaxies on top of the cosmological expansion of the Universe. They have been considered for standard siren measurements ([15] and references therein), but only as a source of systematic uncertainty or bias, since their contribution to the observed galaxies' redshift needs to be subtracted in order to recover the redshift due to the Hubble flow, which is what is needed in a standard siren measurement of the Hubble constant or the Hubble parameter. On the other hand, peculiar velocities also carry important cosmological information, since they follow the inhomogeneous clustering of large scale structure and the laws of gravity. In other words, the peculiar velocity field is a probe of large-scale structure, of its growth, and of the laws of gravity. There exist multiple ways of measuring the peculiar velocity field, for example through redshift space distorsions (RSD), since peculiar velocities distort correlations amongst galaxies along the line of sight. Another possibility is to consider galaxies with a distance estimate, so that the Hubble flow at that distance is known (for a given cosmology) and the peculiar motion can be measured. Distance estimates can be recovered, amongst other methods, through the fundamental plane relation for elliptical galaxies, the Tully-Fisher relation for spiral galaxies, or using Supernovae Type Ia. In [19] we suggest to apply a similar method to measure the peculiar velocity field using the distance estimate provided by gravitational wave sources, where an EM counterpart is available to identify a unique host galaxy. We therefore consider the primary sources of GW and EM emission for existing and upcoming GW experiments, binary neutron star mergers. Current-generation GW detectors do not typically provide BNS distance estimates below the $\sim 10\%$ precision, and they are not expected to be sensitive to BNS mergers beyond ~ 300 Mpc. We thus concentrate our analysis to sources from next-generation gravitational-wave experiments, such as the Einstein Telescope (ET [20]) and the Cosmic Explorer (CE), which are expected to detect nearly all binary neutron star mergers in the Universe and will provide distance estimates as precise as a few per cent at the lowest redshifts.

In order to produce forecasts for the proposed method, we use the peculiar velocity power spectrum, the overdensities power spectrum, and their cross-correlation. The amplitude of overdensities scales with the growth factor D, whose evolution is governed by the linear growth rate $f \equiv \frac{\mathrm{d}\ln D}{\mathrm{d}\ln a}$. The velocity field scales with the overdensity field with a factor f, because of the conservation of mass. The peculiar velocity power spectrum is therefore related to the overdensity power spectrum (in our work, we fix it at the time of the CMB) as $P_{vv} \propto (fD\mu)^2 P_{\delta\delta}(z = \mathrm{CMB})$. The growth of the structure also depends on gravity: the linear growth rate scales as $f \approx \Omega_{\mathrm{m}}^{\gamma}$ for several gravity models, where γ is the growth index, and it depends on gravity [21, 22]. For General Relativity (GR), and two popular gravity models, $f(R)$, and DGP gravity, $\gamma = 0.55, 0.42, 0.68$, respectively [21,22]. It is therefore interesting to constrain γ with a precision of $\sigma_\gamma/\gamma < 20\%$ at 3σ (*i.e.*, $3\sigma_\gamma \sim 0.1$) to be able to discern between GR and the aforementioned gravity models at $\sim 99\%$ confidence level (CL). Finally, the peculiar velocity power spectrum probes gravity through γ as

$$fD = a_{\mathrm{CMB}}\Omega_{\mathrm{m}}^{\gamma}\mathrm{e}^{\int_{a_{\mathrm{CMB}}}^{a}\Omega_{\mathrm{m}}^{\gamma}\mathrm{d}\ln a}, \tag{1}$$

where $\Omega_{\mathrm{m}}(a)$ is the matter density at a time t when the Universe scale factor is $a(t)$. Given the relation between the peculiar velocity power spectrum and the overdensity

power spectrum, the latter will also be sensitive to fD and to the growth index, and so will their cross-correlation.

The same galaxies used for the estimating the peculiar velocity power spectrum, can also be used as tracers of the Universe's mass overdensities to estimate the overdensity power spectrum. Because the number density of GW sources is much lower than that of upcoming galaxy surveys like the Dark Energy Spectroscopic Instrument (DESI [23]) and TAIPAN [24], we also consider cases where the overdensity power spectrum is estimated through the DESI and TAIPAN galaxies, while the peculiar velocity field comes from the GW sources (with measurements of the host galaxy redshift that could also come from the same galaxy surveys). We use a Fisher matrix formalism to derive expected constraints on fD and γ.

3˙1. *Growth of structure.* – First, we compute the expected constraints on the growth of structure assuming GR, so the growth index is fixed to 0.55. We normalize the growth to the amplitude of clustering today, such that $D(z) = \sigma_8(z)$, and a constraint on fD is easily translated into a constraint on $f\sigma_8$. Our results for a 10 year Einstein Telescope experiment with the configuration of [25] are $\sigma(f\sigma_8)/f\sigma_8 = 0.0513,\ 0.0485,\ 0.0921$ at $z = 0.05,\ 0.15$ and 0.25, respectively. These results become even more competitive when they are combined with the galaxies from DESI and TAIPAN for the overdensity power spectrum, and they reach a $\sim 3\%$ precision at $z < 0.2$, as shown by the dark triangles labeled ET BNS + TAIPAN/DESI in fig. 3. These constraints are competitive

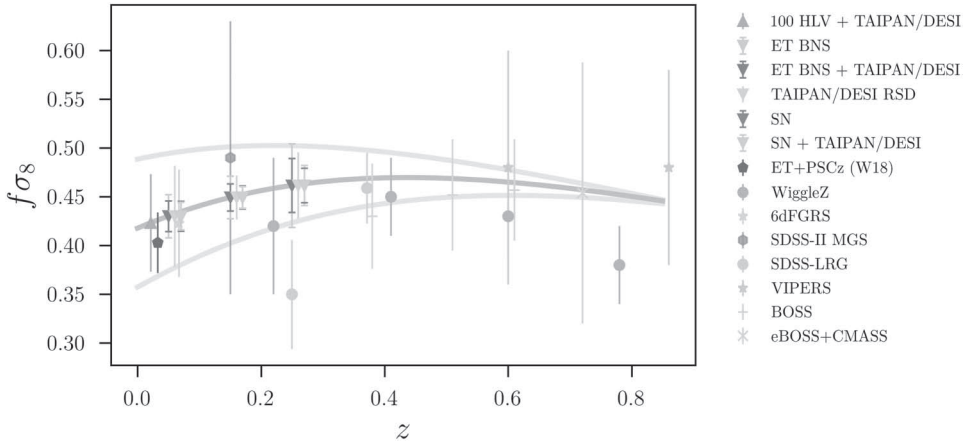

Fig. 3. – Expected constraints on the growth of large-scale structure parameters $f(z)\sigma_8(z)$ using peculiar velocities from host galaxies of gravitational-wave events, assuming a 10-year GW experiment made of 1 Einstein telescope. When the peculiar velocity power spectrum using the GW hosts is combined with the overdensity power spectrum using galaxies from DESI BGS+TAIPAN, we expect to obtain the constraints shown by the dark traingles, computed in 3 redshift bins out to $z < 0.3$. These constraints are competitive with those we expect from a 10 year SN survey. All the results represented by triangles are computed in [19]. The remaining data points represent existing $f(z)\sigma_8(z)$ measurements from 6dF [26], WiggleZ [27], SDSS-II LRG [28], SDSS-II Main Galaxy sample [29], BOSS [30], VIPERS [31] and eBOSS-CMASS [32]. We also report the forecast from [33] (black pentagon), who use a combination of GW and PSCz galaxy survey data. The darker line is the theoretical prediction for $f(z)\sigma_8(z)$ in a Flat ΛCDM Universe with $\gamma = 0.55$ (GR), while the other curves show the theoretical prediction from $\gamma = 0.42$ and $\gamma = 0.68$ (which are the values predicted for $f(R)$ and DGP gravity, respectively).

with those we expect for a 10 year Supernova (SN) survey covering half of the sky, and they significantly improve upon the DESI/TAIPAN-only constraints on $f\sigma_8$ at $z < 0.2$, making the proposed probe with GW sources promising. Similar constraints can also be recovered by a shorter GW experiment if a multiple detector network becomes available (*e.g.*, ~ 5 years for a 2 ET and 1 CE network).

3˙2. *Testing General Relativity.* – Next, we let the growth index free and explore our expected ability to constrain it with a 3G GW experiment. The darker line in fig. 3 is the theoretical prediction for $f(z)\sigma_8(z)$ in a Flat ΛCDM Universe with $\gamma = 0.55$ (GR), while the other curves show the theoretical prediction from $\gamma = 0.42$ and $\gamma = 0.68$ (which are the values predicted for $f(R)$ and DGP gravity, respectively). From the figure, it is clear that our ability to constrain gravity models with GW sources and peculiar velocities should be useful in discerning different values of γ, and therefore, different gravity models.

Figure 4 shows our forecasted uncertainty on γ for different values of the luminosity distance precision σ_{d_*}/d_* and of the BNS volumetric rates integrated over time, considering events out to $z_{\rm max} < 0.3$. The results are valid for a 5 year GW experiment, assuming the maximum *a posteriori* BNS rate of [34]. If the true value of the rate is closer to the lower limit of the [34] 90% CI constraint, a longer time will be needed to achieve the same results, and vice versa, if the true value of the rate is higher, better constraints can be achieved in the 5-year time frame. The white stars in fig. 4 show the extent of this rate variation. The value of σ_{d_*} is the luminosity distance uncertainty recovered

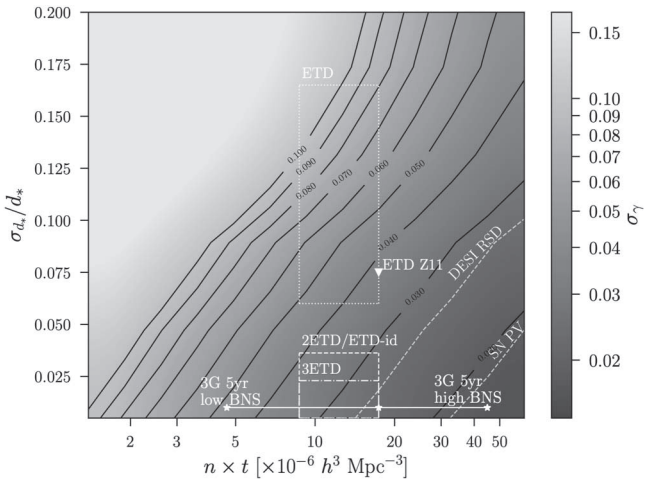

Fig. 4. – Expected constraints on the growth index γ from peculiar velocity measurements using BNS mergers from a 5-year 3G GW experiment. The constraints, shown by the gradient, are plotted for different values of the distance precision, and as a function of BNS volumetric rates integrated over time, considering events out to $z_{\rm max} < 0.3$. The distance uncertainty σ_{d_*} is the uncertainty at a distance d_*, which corresponds to $z_* = 0.1$. The BNS volumetric rate assumed is the maximum *a posteriori* value from [34] ($1.09 \times 10^{-6} \times (h/0.679)^3$ Mpc^{-3} yr^{-1}). The low and high 90% CI limits on the rate are shown by the stars for a 5-year 3G GW experiment having a distance precision of 1% at d_*. The various boxes represent the regions of parameter space where we expect future constraints to fall assuming various ET configurations. The white triangle represents our expectations assuming the [25] approximation for 1 ET. We also show the constraints expected for DESI RSD and for an LSST-like SN survey as in [35] (grey dashed lines). Adapted from [19].

from the GW data at a reference distance d_* corresponding to $z = 0.1$. The uncertainty σ_{d_*} for each GW event scales with the event distance, and more distant events have a worse precision. This is the reason why we only consider events thorugh $z_{\rm max} < 0.3$, but our analysis shows that most of the constraining power for both the growth index and the $f\sigma_8$ constraints comes from sources at $z < 0.2$ (as clear also from comparing the constraints of fig. 3 in the first two redshift bins to the third one).

As mentioned above, an interesting constraint on γ is one that lets us discern between the gravity models predictions with a 3σ confidence, and that is possible if $\sigma_\gamma < 0.04$. We therefore want to be in the bottom right portion of fig. 4, below the 0.04 black line. Our results show that this constraint will be achieved with a 1 ET 5-year experiment with the configuration of [25] (white triangle), and that a network made of 2 or 3 ET can potentially reach a 0.03 precision on the growth index. This constraint can be improved down to $\sigma_\gamma \sim 0.02$ when combined with galaxy overdensities. Our results are competitive with other expected constraints, *e.g.*, from DESI RSD and SNe peculiar velocity, and are complementary to those probes. Our method is complementary to DESI RSD as the constraints on the growth index are recovered from a lower redshift range, and the complementarity is similar to that expected for peculiar velocities from SNe Ia, as explained in detail in [35]. Gravitational waves also offer complementary measurements to SNe: in the nearby Universe, 3G GW detectors are expected to reach a distance precision that is not possible for SNe Ia because of their intrinsic scatter, and can therefore be used to create the most precise maps of the nearby Universe.

4. – Conclusions

Synergies between large galaxy surveys and gravitational-wave experiments provide extremely promising avenues to measure cosmological parameters. First, large galaxy surveys are able to provide the positions of a large number of potential host galaxies for a GW event, therefore providing the first ingredient necessary to optimize follow-up strategies and increase the chances of finding electromagnetic counterparts. A large galaxy survey, the DES, was in fact one of the collaborations that was able to discover the first optical counterpart to a gravitational-wave event [2, 36], and counterparts are extremely valuable to recover cosmological parameters through the bright standard siren method. Secondly, the same galaxies from large sky surveys can be used to infer cosmological parameters through the dark standard siren method for GW events without an electromagnetic counterpart. Using LIGO/Virgo GW events, DES galaxies, and the information available from the EM counterpart to GW170817, we present a state-of-the-art standard siren measurement in [16], where we show that dark standard sirens can provide significant improvement to bright standard sirens in the measurement of the Hubble constant H_0, yielding $H_0 = 72.0^{+12}_{-8.2}$ km s^{-1} Mpc^{-1}, provided that a complete and uniform galaxy catalog is available at the location of the dark sirens. Using events from the next LIGO/Virgo observing run, starting in $\sim$ 2022, we expect that a 2–5% statistical precision on H_0 will be achieved from dark sirens only once $\mathcal{O}(100)$ nearby (at a luminosity distance < 900 Mpc) are detected. In combination with bright standard siren measurements of the Hubble constant from the same upcoming run, we expect standard sirens to be a promising probe to shed light on the Hubble constant tension in the coming years.

Future GW experiments also present the possibility of using GW sources to measure the peculiar velocity field, derive constraints on the growth of large scale structure, and test General Relativity. In [19] we show that data from a 10 year run of the Einstein

Telescope, together with galaxies' redshifts from DESI and TAIPAN (or any other spectroscopic galaxy survey providing redshifts for a similar number density of galaxies in the Northern and Souther hemispheres), will provide a $\sim 3\%$ precision measurement of $f\sigma_8$. Moreover, data from a 5-year ET experiment (with the host galaxies' redshifts) will be able to constrain the growth index to $\sigma_\gamma < 0.04$, which will allow us to confidently test General relativity and make a distinction with other popular gravity models at the $\sim 3\sigma$ level.

As we prepare for the future of gravitational waves with next-generation GW detectors, it is important that we exploit currently available GW data, while identifying the needs of the next-stage Dark Energy experiments and digital sky surveys, which would extremely benefit by the addition of standard sirens and multi-messenger probes.

* * *

The author acknowledges all DES, DESI, LIGO and Virgo collaborators, who have played a crucial role in the analyses presented here. Work supported by the Fermi National Accelerator Laboratory, managed and operated by Fermi Research Alliance, LLC under Contract No. DE-AC02-07CH11359 with the U.S. Department of Energy. The U.S. Government retains and the publisher, by accepting the article for publication, acknowledges that the U.S. Government retains a non-exclusive, paid-up, irrevocable, world-wide license to publish or reproduce the published form of this manuscript, or allow others to do so, for U.S. Government purposes.

REFERENCES

[1] LIGO Scientific Collaboration, Virgo Collaboration, GBM F., INTEGRAL, IceCube Collaboration, AstroSat Cadmium Zinc Telluride Imager Team, IPN Collaboration, The Insight-Hxmt Collaboration, ANTARES Collaboration, The Swift Collaboration, AGILE Team, The 1M2H Team, The Dark Energy Camera GW-EM Collaboration, the DES Collaboration, The DLT40 Collaboration, GRAWITA (GRAvitational Wave Inaf TeAm), The Fermi Large Area Telescope Collaboration, ATCA (Australia Telescope Compact Array) ASKAP (Australian SKA Pathfinder) Las Cumbres Observatory Group, OzGrav, DWF, AST3, CAASTRO Collaborations, The VINROUGE Collaboration, MASTER Collaboration, J-GEM, GROWTH, JAGWAR, NRAO C., TTU-NRAO, NuSTAR Collaborations, Pan-STARRS, The MAXI Team, Consortium T., KU Collaboration, Optical Telescope N., ePESSTO, GROND, Tech University T., SALT Group, TOROS (Transient Robotic Observatory of the South Collaboration), The BOOTES Collaboration, MWA (The Murchinson Widefield Array) The CALET Collaboration, IKI-GW Follow-up Collaboration, H. E. S. S. Collaboration, LOFAR Collaboration, LWA (Lone Wavelength Array) HAWC Collaboration, The Pierre Auger Collaboration, ALMA Collaboration, Euro VLBI Team, Pi of the Sky Collaboration, The Chandra Team at McGill University, DFN (Desert Fireball Network) ATLAS, Time Resolution Universe Survey H., RIMAS, RATIR and South Africa/MeerKAT S., *Astrophys. J.*, **848** (2017) L12.
[2] Soares-Santos M. *et al.*, *Astrophys. J.*, **848** (2017) L16.
[3] Abbott B. P. *et al.*, *Nature*, **551** (2017) 85.
[4] Palmese A. *et al.*, *Astrophys. J.*, **849** (2017) L34.
[5] Palmese A. and Conselice C. J., *Phys. Rev. Lett.*, **126** (2021) 181103, arXiv:2009.10688.
[6] Tsai Y.-D., Palmese A., Profumo S. and Jeltema T., *Is gw170817 a multimessenger neutron star-primordial black hole merger?*, arXiv:2007.03686 (2020).

[7] Schutz B. F., *Nature*, **323** (1986) 310.
[8] Feeney S. M., Peiris H. V., Williamson A. R., Nissanke S. M., Mortlock D. J., Alsing J. and Scolnic D., *Phys. Rev. Lett.*, **122** (2019) 061105.
[9] Palmese A. *et al.*, *BAAS*, **51** (2019) 310.
[10] The Dark Energy Survey Collaboration, preprint, arXiv:astro-ph/0510346 (2005).
[11] Soares-Santos M., Palmese A. *et al.*, *Astrophys. J.*, **876** (2019) L7.
[12] Abbott B. P. *et al.*, *Phys. Rev. Lett.*, **119** (2017) 141101.
[13] Abbott R., Abbott T. D., Abraham S., Acernese F., Ackley K., Adams C. and Adhikari R. X., *Astrophys. J.*, **896** (2020) L44.
[14] Morgan R. *et al.*, *Astrophys. J.*, **901** (2020) 83.
[15] Nicolaou C., Lahav O., Lemos P., Hartley W. and Braden J., *Mon. Not. R. Acad. Sci.*, **495** (2020) 90.
[16] Palmese A. *et al.*, *Astrophys. J.*, **900** (2020) L33.
[17] Singer L. P. and Price L. R., *Phys. Rev. D*, **93** (2016) 024013.
[18] Chen H.-Y., Fishbach M. and Holz D. E., *Nature*, **562** (2018) 545.
[19] Palmese A. and Kim A. G., *Phys. Rev. D*, **103** (2021) 103507, arXiv:2005.04325.
[20] Punturo M. *et al.*, *Class. Quantum Grav.*, **27** (2010) 194002.
[21] Linder E. V., *Phys. Rev. D*, **72** (2005) 043529.
[22] Linder E. V. and Cahn R. N., *Astropart. Phys.*, **28** (2007) 481.
[23] DESI Collaboration, arXiv:1611.00036 (2016).
[24] da Cunha E. *et al.*, *Publ. Astron. Soc. Aust.*, **34** (2017) E047.
[25] Zhao W., Van Den Broeck C., Baskaran D. and Li T. G. F., *Phys. Rev. D*, **83** (2011) 023005.
[26] Beutler F. *et al.*, *Mon. Not. R. Astron. Soc.*, **423** (2012) 3430.
[27] Blake C. *et al.*, *Mon. Not. R. Astron. Soc.*, **415** (2011) 2876.
[28] Oka A., Saito S., Nishimichi T., Taruya A. and Yamamoto K., *Mon. Not. R. Astron. Soc.*, **439** (2014) 2515.
[29] Howlett C., Ross A. J., Samushia L., Percival W. J. and Manera M., *Mon. Not. R. Astron. Soc.*, **449** (2015) 848.
[30] Satpathy S. *et al.*, *Mon. Not. R. Astron. Soc.*, **469** (2017) 1369.
[31] de la Torre S. *et al.*, *Astron. Astrophys.*, **608** (2017) A44.
[32] Icaza-Lizaola M. *et al.*, *Mon. Not. R. Astron. Soc.*, **492** (2020) 4189.
[33] Wang Y. Y., Wang F. Y. and Zou Y. C., *Phys. Rev. D*, **98** (2018) 063503.
[34] The LIGO Scientific Collaboration and the Virgo Collaboration, arXiv:2001.01761 (2020).
[35] Kim A. G. and Linder E. V., *Phys. Rev. D*, **101** (2020) 023516.
[36] Herner K. *et al.*, *Astron. Comput.*, **33** (2020) 100425.